

In Vitro Evaluation of Textile Chitosan Scaffolds for Tissue Engineering using Human Bone Marrow Stromal Cells

Christiane Heinemann,* Sascha Heinemann, Anja Lode, Anne Bernhardt, Hartmut Worch, and Thomas Hanke

Max Bergmann Center of Biomaterials and Institute of Materials Science, Dresden University of Technology, Budapester Strasse 27, D-01069 Dresden, Germany

Received February 9, 2009; Revised Manuscript Received March 5, 2009

Textile chitosan fiber scaffolds were developed and tested in terms of biocompatibility for human bone marrow stromal cells (hBMSCs). A part of the scaffolds was further modified by coating with fibrillar collagen type I in order to biologize the surface. hBMSCs of two donors were used for cell culture experiments in vitro. Confocal laser scanning microscopy (CLSM) as well as scanning electron microscopy (SEM) revealed fast attachment and morphological adaptation of the cells on both the raw chitosan fibers and the collagen-coated scaffolds. Cells were osteogenically induced after 3 days and cultivated for up to 28 days on the scaffolds. Activity of lactate dehydrogenase (LDH) and alkaline phosphatase (ALP) was analyzed to evaluate proliferation as well as osteogenic differentiation. We found a 3.5–6-fold increase in the cell number, whereas the collagen coating did not noticeably influence these factors. Osteogenic differentiation was confirmed by the course of ALP activity and immunostaining of osteocalcin. The feature of the collagen-coated as well as the raw chitosan fiber scaffolds to support attachment, proliferation, and differentiation of hBMSCs suggests a potential application of chitosan fibers and textile chitosan scaffolds for the tissue engineering of bone.

Introduction

The focus of bone tissue engineering research is nowadays on third-generation biomaterials, which are characterized to support self-healing processes of the tissue concerned.^{1,2} In this field, the polysaccharide chitosan has attracted attention because of its inherent biocompatibility, biodegradability, osteoconductivity, and cost-effective availability.³ Furthermore, the presence of functional residues facilitates chemical modification of the material, resulting in various derivatives.⁴ In vivo, degradation by lysozymes is recognized to hydrolyze chitosan, resulting in the formation of nontoxic oligomers.^{5–7} Recent studies revealed degradation products of chitosan to support angiogenesis.⁸ In contrast, the degradation of synthetic polymers such as polyglycolic acid (PGA), poly-L-lactide (PLLA), and poly(lactico-glycolic acid) (PLGA) generates acid products, which often cause inflammation.⁹

Chitosan is a copolymer of *N*-acetyl-glucosamine and *N*-glucosamine units and is produced by deacetylation of naturally occurring chitin, which is extracted from shellfish sources.¹⁰ When the percentage of *N*-acetyl-glucosamine units is lower than 50%, the term chitosan is used. Because of its solubility in dilute acids, chitosan is accessible for various established processing technologies (e.g., freeze-drying, freeze-gelation) and has been used to produce films, gels, as well as porous sponge-like scaffolds.^{11,12} For two decades, chitosan has become a frequently applied material in regenerative medicine and biomaterials research including orthopedics, periodontology, drug delivery systems, wound healing applications, and tissue engineering.^{13–15}

New perspectives in tissue engineering scaffold design were introduced by the availability of processable polymer fibers. In the case of chitosan, fibers are produced by the electro-spinning

or wet-spinning process.¹⁶ In the latter case, the polymer is dissolved in an acid solvent and then extruded into a nonsolvent, which precipitates the fibers. The application of established textile techniques enables the production of two- (2D) and three-dimensional (3D) scaffolds, which are featured by significant advantages over conventional sponge/foam-like scaffolds. Most important are higher porosity, degradability, and ratio of surface area to volume, which is known to support the adhesion of cells and the diffusion of nutrients inside the scaffold.¹⁷ Furthermore, controlled arrangement of the scaffold fibers allows realization of adapted anisotropic mechanical properties.¹⁸

Because of the numerous advantages, processing chitosan fibers into textile scaffolds for tissue engineering applications is obviously an innovative and promising topic. However, until now, only few studies report on the usage of textile structures from pure chitosan — mostly conventional scaffold materials are slightly modified by the introduction of chitosan fibers.¹⁹

Previously, we described the development of novel scaffold models made of chitosan fibers.²⁰ Coating with a thin layer of fibrillar collagen type I was applied to biologize the surface of the scaffolds, but did not further improve the remarkable biocompatibility of the unmodified chitosan fiber scaffolds. The first cell culture experiments using a murine cell line of osteoblast-like cells (7F2) revealed fast cell attachment, considerable increase of the cell number over the cultivation period of 28 d, and the expression of the osteogenic phenotype as indicated by the typical pattern of ALP activity, osteocalcin immunostaining, and matrix mineralization.²⁰

Motivated by the excellent suitability of the novel chitosan fiber scaffolds for the expansion and differentiation of murine osteoblasts, corresponding experiments had to be performed with cells of human origin with regard to a potential application in bone tissue engineering. Bone marrow stromal cells, also referred to as mesenchymal stem cells (MSCs), play a pivotal role in bone regeneration and repair in vivo.^{21,22} The cells are

* To whom correspondence should be addressed. E-mail: christiane.heinemann@tu-dresden.de.

able to differentiate along the osteogenic and various other cell lineages, and the capability of self-replication allows their extensive expansion *in vitro*.^{23–25} These properties make MSC ideal candidates for tissue engineering applications.²⁶

In the present study, human bone marrow stromal cells (hBMSCs) were seeded and cultivated on uncoated and collagen-coated chitosan fiber scaffolds for 28 d with and without osteogenic supplements. Adhesion, proliferation, and osteogenic differentiation were investigated.

Materials and Methods

Chitosan Fiber Scaffolds and Collagen Coating. Wet-spun chitosan fibers were provided in the form of a multifilament yarn by Heppe GmbH, Germany. The raw material is crab chitin which is deacetylated (DD 90%) to chitosan of molecular weight between 100 000 and 200 000 g·mol⁻¹. For microscopic analyses, the chitosan fibers were tightened between the plastic rings of Minusheet holders (inner diameter 10 mm) (Minucells, Bad Abbach, Germany). Stand-alone scaffolds (diameter 10 mm) for quantitative biochemical analyses were processed by using the crown knot technique.²⁰

Bovine tropocollagen type I (Invitrogen, Carlsbad, USA) was assembled into a fibrillar coating directly on the scaffolds as described previously.²⁰ In brief, the chitosan scaffolds were soaked in a mixture of tropocollagen solution and physiological buffer solution at 4 °C. Fibrillogenesis was carried out at 37 °C, followed by rinsing and lyophilization. The collagen coating was stabilized by chemical cross-linking using *N*-(3-dimethylaminopropyl)-*N'*-ethylcarbodiimide (EDC) and *N*-hydroxysuccinimide (NHS) (both Sigma, Taufkirchen, Germany).

Gamma-irradiation (25 kGy) was used to sterilize the uncoated and collagen-coated chitosan scaffolds before starting the cell culture experiments.

Cell Culture. hBMSCs, isolated from bone marrow aspirates of two donors (donor I: 33 years old, donor II: 31 years old) as described, were kindly provided by Prof. Bornhäuser and co-workers, Medical Clinic I, Dresden University Hospital.²⁷ The cells were expanded in Dulbecco's modified Eagle's medium (DMEM), low glucose, supplemented with 10% fetal calf serum (FCS), 10 U/mL penicillin and 100 µg/mL streptomycin in a humidified atmosphere at 37 °C and 7% CO₂. Cells in passage 5 were used for the experiments. Medium and all supplements were obtained from Biochrom, Berlin, Germany.

The scaffolds were placed in 48-well-plates and soaked in cell culture medium for 24 h in order to prevent floating. After removing the medium, 40 µL of cell suspension (5000 cells per µL) were placed onto each scaffold. Cells were allowed to adhere for 30 min in the incubator before filling up the wells with additional medium. On the third day, cells were osteogenically induced by addition of 100 nM dexamethasone (Sigma, Taufkirchen, Germany), 50 nM ascorbic acid 2-phosphate (Sigma), and 7.4 mM β-glycerophosphate (Sigma) to the medium.²⁸ The medium was changed twice weekly.

Microscopy. Scanning electron microscopy (SEM) was used to characterize the uncoated and collagen-coated chitosan scaffolds before and after cell culture experiments, respectively. Preparation of the cell-seeded samples was described previously.²⁰ In brief, the samples were washed and the cells were fixed. After dehydration and critical-point drying, the samples were mounted on stubs and sputtered with gold. Microscopy was carried out using a Philips ESEM XL 30 in Hi-Vac mode by applying an acceleration voltage of 3 kV and detecting secondary electrons for imaging. Additionally, energy dispersive X-ray (EDX) mapping was performed in order to visualize distribution of calcium and phosphorus as typical elements of cell-formed mineral.

Confocal laser scanning microscopy (CLSM) was applied to evaluate cell morphology, orientation, growth, and differentiation. After washing and fixing, the cells were permeabilized with 0.2% Triton-X-100 in PBS and blocked with 1% bovine serum albumin (BSA, Sigma) for 30 min. Cytoskeletal actin was stained with AlexaFluor 488-Phalloidin (Invitrogen), cell nuclei with 4',6-diamidino-2-phenylindole (DAPI,

Sigma). In the case of collagen-coated chitosan fibers, antibovine collagen type I (mouse IgG) (Sigma) was linked to the collagen coating. AlexaFluor 546 conjugated goat antimouse IgG (Invitrogen) was used as the secondary antibody for staining. In order to visualize differentiation behavior, ALP was stained using the ELF97 Endogenous Phosphatase Detection Kit (Invitrogen). Osteocalcin was labeled with antihuman osteocalcin (goat IgG) (Santa Cruz Biotechnology, USA), followed by staining with AlexaFluor 488 conjugated donkey anti-goat IgG (Invitrogen). The cytoskeletal Actin was stained with AlexaFluor 546-Phalloidin. Collagen was not stained in that case. Microscopy was carried out on an upright Axioscop 2 FS mot equipped with a LSM 510 META module (Zeiss, Jena, Germany) controlling an argon-ion (Ar⁺) laser, helium–neon (HeNe) laser and NIR-femtosecond titanium-sapphire laser for 2-photon excitation (Coherent Mira 900F). Excitation of AlexaFluor 488 was carried out at 488 nm (Ar⁺ laser), the excitation of AlexaFluor 546 at 546 nm (HeNe laser). The NIR-fs-laser laser was used for excitation of DAPI at 750 nm (2 photon excitation) and fluorescence was recorded at 461 nm.

Colorimetric Measurements. Examination of proliferation and osteogenic differentiation were carried out by a lactate dehydrogenase (LDH) assay and an alkaline phosphatase (ALP) assay, respectively. All measurements were performed with cell lysates obtained after 1, 3, 7, 10, 14, 21, and 28 days of cultivation. Cell lysis was achieved with 1% Triton X-100 (Sigma) in phosphate-buffered saline (PBS). Ultrasonication (20 s, 80 W) of the scaffolds was applied to support cell lysis. For all colorimetric measurements, a SpectraFluor Plus microplate reader (Tecan, Crailsheim, Germany) was used.

LDH Activity Assay. Cell proliferation was determined through the total activity of LDH in the cell lysates using an LDH Cytotoxicity Detection Kit (Takara, Saint-Germain-en-Laye, France). An aliquot of cell lysate was mixed with LDH substrate buffer, and the enzymatic reaction was stopped after 30 min with 0.5 M HCl. The absorbance was read at 492 nm. The LDH activity was correlated with the cell number using a calibration line of cell lysates with defined cell number.^{29,30}

ALP Activity Assay. Cell differentiation was evaluated by the measurement of ALP activity. An aliquot of cell lysate was added to ALP substrate buffer, containing 2 mg/mL p-nitrophenyl phosphate (Sigma), 0.1 M diethanolamine, 1 mM MgCl₂, 0.1% Triton X-100 (pH 9.8), and the mixture was incubated at 37 °C for 30 min. The enzymatic reaction was stopped by the addition of 0.5 M NaOH, and the absorbance was read at 405 nm. A calibration line was constructed from different concentrations of p-nitrophenol.

Statistics. All measurements were collected in triplicate and expressed as means ± standard deviations. Student's *t* test was employed to assess the statistical significance of results. *P* values less than 0.05 were considered significant for all analyses.

Results

Adhesion, proliferation and differentiation analyses of hBMSC cultivated on chitosan fibers were carried out using two scaffold models.²⁰ Supported chitosan scaffolds form a smooth surface of parallel aligned fibers suitable for microscopic investigations (Figure 1a). Stand-alone chitosan scaffolds of the same material were used for biochemical assays (Figure 1b). The raw fibers show slightly edged cross sections and diameters of about 20 µm (Figure 1c). Collagen coating results in the formation of smooth layers at the surface and inside the scaffold by spanning over several chitosan fibers (Figure 1d).

Cell Adhesion and Proliferation. Cell adhesion on the uncoated and on the collagen-coated chitosan scaffolds was monitored by microscopy. CLSM visualizes the spreading of the green fluorescent actin skeleton, which characterizes the adaptation of the cells to the given substrate (Figure 2a,b). Additionally, cell nuclei are visualized by blue color and collagen coating by a red staining.

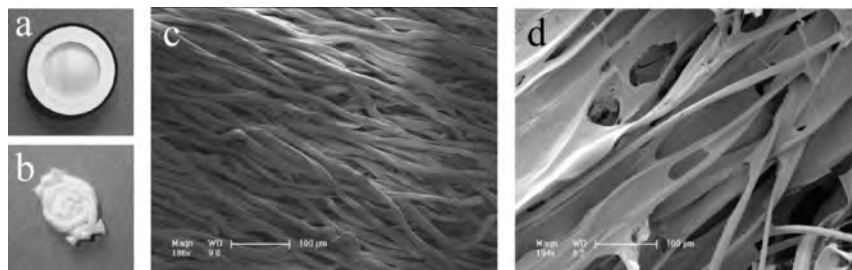


Figure 1. Photographs of the supported (a) and stand-alone (b) chitosan scaffolds. SEM images show the uncoated (c) and collagen-coated (d) chitosan scaffolds.

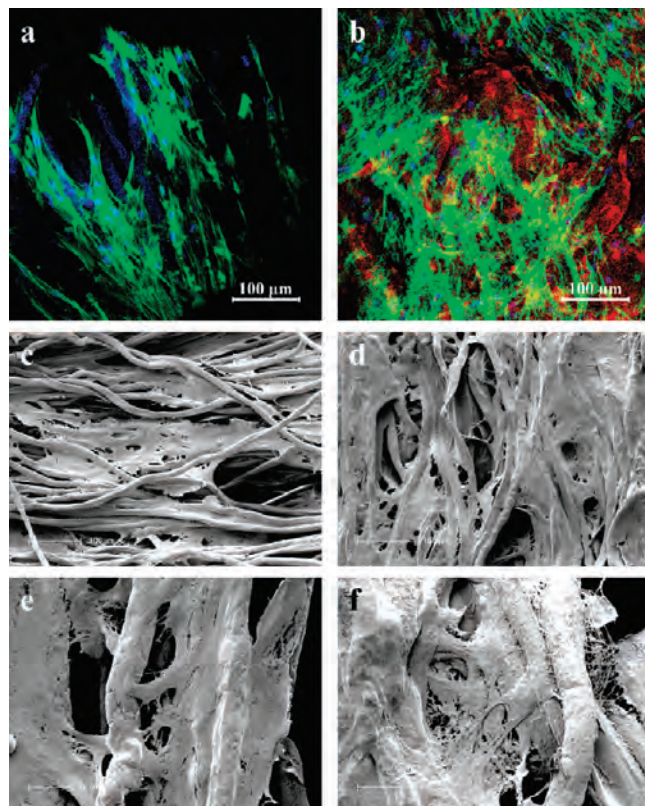


Figure 2. 3D reconstructions from CLSM image stacks of hBMSCs after 24 h of cultivation on uncoated (a, left column) as well as collagen-coated (b, right column) chitosan scaffolds. The actin skeletons (green), the nuclei (blue), and the collagen (red) are visible. Panels c–f show corresponding SEM images of exactly the same samples.

After 24 h, the cells are completely spread along the fibers of the uncoated chitosan scaffold. At suitable sites the cells evenly span over several single fibers, which emphasizes the remarkable adaptability of the cells to the given substrate. The image highlights preferred spreading toward the fiber's alignment to achieve the maximal contact area. For the collagen-coated scaffolds, the alignment is more irregular, and cell patches enveloping the coated chitosan fibers are visible. SEM images of exactly the same samples simultaneously visualize the morphology of both the cells and the fibers (Figure 2c–f). Cell patches are easy to identify on the uncoated scaffold. For the coated scaffolds, cells exhibit a rough surface compared to the collagen.

Proliferation of the hBMSC was quantitatively determined over a cultivation period of 28 d and is illustrated in Figure 3. HBMSC and osteogenically induced hBMSC showed good proliferation rates on both raw and collagen-coated chitosan scaffolds. On the supposition of constant LDH activity per

cell during the whole cultivation period, the initial cell numbers of noninduced hBMSC increased by factors of about 2.6 (donor I) and about 2 (donor II) on both the uncoated and collagen-coated scaffolds after 28 d of cultivation. For osteogenically induced hBMSCs, cell numbers on uncoated and collagen-coated increased about 6-fold (donor I) and 3.5-fold (donor II), respectively.

The cell number on the collagen-coated scaffolds (e.g., about 45 000 at day 1 for donor I) at the early time points of cultivation is slightly but significantly higher than that on the uncoated scaffolds (e.g., about 40 000 at day 1 for donor I). Later on, no significant differences are detected for osteogenically induced as well as for noninduced cells.

For both scaffold types, the osteogenically induced cells show higher proliferation rates compared to noninduced cells. That is also noticed for the cultivation on polystyrene culture dishes (Supporting Information).

After 14 d of cultivation, proliferation of the osteogenically induced hBMSC on the uncoated and collagen-coated chitosan scaffolds was visualized by CLSM and SEM. Figure 4 confirms the increase of cell density and the formation of dense layers on both scaffold types, which correlates to the results of the biochemical assay. The chitosan fibers are completely overgrown and distinction between cells and previously deposited collagen is hardly possible.

Cell Differentiation. Differentiation of hBMSCs toward the osteoblastic lineage was analyzed by detection of the typical markers ALP, osteocalcin, and matrix mineralization. The progress of specific ALP activity of the hBMSC with respect to the donor, osteogenic induction, and collagen coating is illustrated in Figure 5.

Innately, all cell fractions show equally low ALP activity until the addition of osteogenic supplements at day 3. During further cultivation, ALP activity of osteogenically induced hBMSC raises both on coated and uncoated chitosan scaffolds, whereas the ALP activity of the noninduced cells maintains the typical low level over the 28 day cultivation period. In addition to the quantitative determination, ALP activity of osteogenically induced hBMSC at day 14 is visualized by CLSM and is present as yellow dots in Figure 4 a,b.

A different pattern of specific ALP activity was detected for hBMSC of the examined donors. For the osteogenically induced hBMSCs of donor I, the ALP activity increase on both scaffold types starts between days 7 and 10 and reaches the typical maximum around day 14, representing osteogenic differentiation.³¹ Osteogenically induced hBMSCs cultivated on polystyrene culture dishes as a control reach the ALP maximum only around day 21 (Supporting Information).

Specific ALP activity of donor II hBMSC increases similarly as a result of osteogenic induction (starting from day 7, significant from day 10 for the uncoated scaffolds, significant from day 21 for the collagen-coated scaffolds); however, it

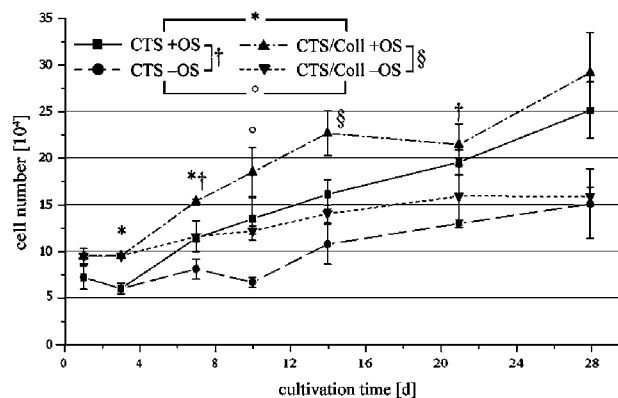
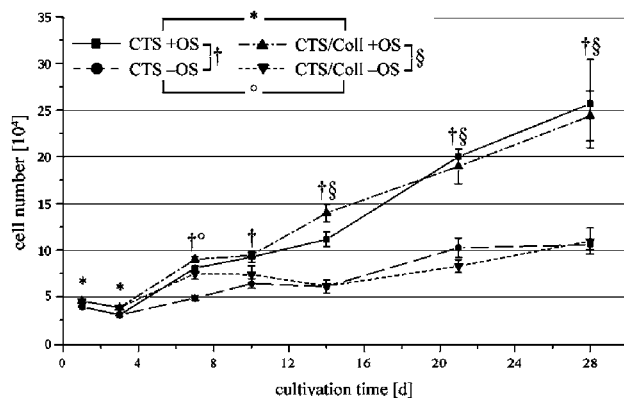


Figure 3. Cell number (calculated from total LDH activity) of noninduced (–OS) and osteogenically induced (+OS) donor I hBMSC (left) and donor II hBMSC (right) cultivated on uncoated (CTS) or collagen-coated (CTS/Coll) chitosan scaffolds. *, †, §: $p \leq 0.05$.

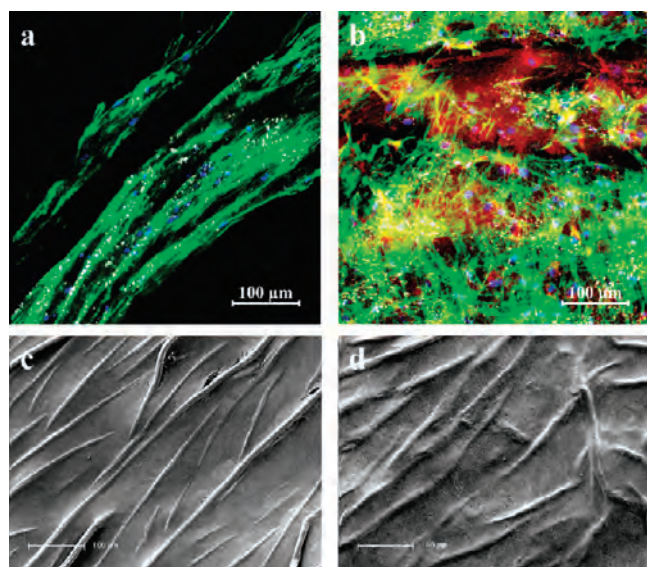


Figure 4. 3D reconstructions from CLSM image stacks of hBMSCs after 14 days of cultivation on uncoated (a, left column) as well as collagen-coated (b, right column) chitosan scaffolds. The actin skeletons (green), the nuclei (blue), the collagen (red), and the ALP activity (yellow) are visible. Panels c and d show corresponding SEM images of exactly the same samples.

continues to increase until day 28. Similar results are obtained for cultivation on control polystyrene culture dishes (Supporting Information). From day 21, the ALP values are slightly higher for the uncoated chitosan scaffolds.

The presence of osteocalcin was verified by immunostaining followed by CLSM. Figure 6a shows the cell nuclei (blue), actin skeletons (red), and osteocalcin (green) of osteogenically induced donor I hBMSCs after 28 days of cultivation on the uncoated chitosan scaffold.

The chitosan fibers occur as dark areas in the image and are enveloped by red fluorescent actin. The green fluorescence shows that osteocalcin is concentrated at the surface of the chitosan fibers. This is also confirmed by sectional planes (Figure 6b). Detection of osteocalcin on the collagen-coated scaffolds is disturbed by autofluorescence of the scaffold. Osteocalcin was not detectable for the noninduced cell fraction (data not shown).

Qualitative analysis of cell mineralization was performed by SEM and EDX spectroscopy. Figure 6c shows the uncoated scaffold after 28 days to be overgrown densely by the osteoblasts. In contrast to the SEM images taken after 14 days of cultivation, mineral was detected, visible as spherical particles

and agglomerates embedded in the extracellular matrix (Figure 6d). Single particles exhibit a size of about 1–2 μm . EDX mapping of the shown areas revealed an increased presence of calcium and phosphorus located at the particles (Supporting Information).

Discussion

The development of scaffolds, to support and regulate bone regeneration by functioning as the fibrillar part of extracellular matrix and maintaining the space and shape of the defect, is still a major concern in tissue engineering research.³² In this field, the biomaterials collagen and chitosan have demonstrated intrinsic properties that favor their application as a base material. In the present study, the potential of uncoated and collagen-coating textile chitosan scaffolds for adhesion, proliferation and differentiation of hBMSC was investigated and is discussed.

Textile techniques facilitated the preparation of chitosan scaffolds exhibiting an ordered structure of bundled fibers whose rough surface is determined by the wet spinning process.^{20,33,34} A coating procedure is well established for the chitosan scaffolds and allows the formation of collagen layers spanning between several fibers.²⁰ Coating tissue engineering scaffolds with collagen is a common procedure to enhance the biocompatibility.^{35–37} The open fiber structure is preserved, and the porosity guarantees nutrient supply as well as cell ingrowth.^{20,32} All cell culture experiments were performed for the uncoated and for the collagen-coated chitosan scaffolds in order to analyze the influence of the biologization. Adhesion, proliferation, and differentiation of osteogenically induced and noninduced hBMSCs of two donors were evaluated.

The combination of cLSM and SEM is particularly suitable to show the morphology, distribution, and orientation of the cells adhered to the uncoated and coated scaffolds. Twenty-four hours after seeding, the cells are flat and spread on both scaffold types, dependent on the morphology of the substrate. Adhesion on the uncoated chitosan scaffolds occurs by alignment in the direction of the chitosan fibers followed by enveloping the cylindrical substrate. Collagen coating changed the scaffold's morphology, and cells were allowed to spread irregularly on the additional surface areas. Determination of the number of cells attached to the substrates 24 h after seeding revealed a slightly higher seeding efficiency for the collagen-coated scaffolds (Figure 3). A positive impact of the collagen-coating on adhesion was also observed in our previous study: microscopic investigations of the attachment of 7F2 osteoblasts showed a more progressed and enhanced cell spreading on the

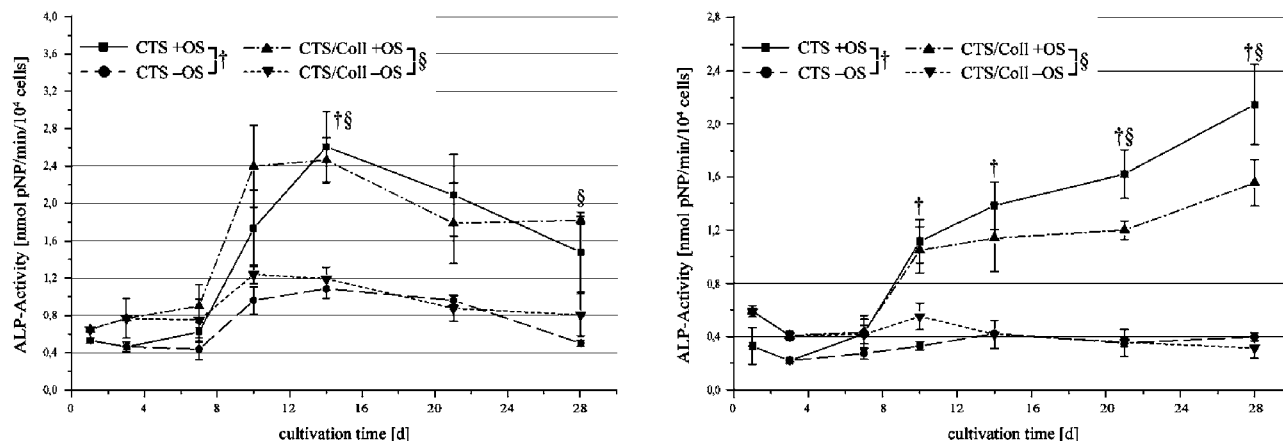


Figure 5. Specific ALP activity (related to cell number) of noninduced (–OS) and osteogenically induced (+OS) donor I hBMSC (left) and donor II (right) hBMSCs cultivated on uncoated (CTS) or collagen-coated (CTS/Coll) chitosan scaffolds. †, §: $p \leq 0.05$.

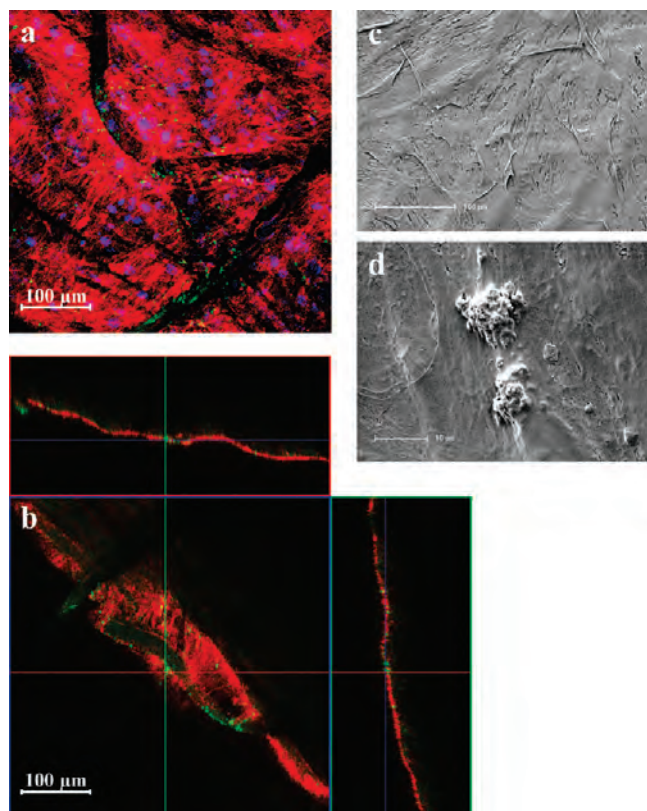


Figure 6. 3D reconstruction from 15 CLSM images of osteogenically induced donor I hBMSCs after 28 days of cultivation on the uncoated chitosan scaffolds (a). *ortho*-Representation showing a single image of the stack and cross sections along the colored lines (b). The actin skeletons (red), the nuclei (blue), and the osteocalcin (green) are visible. Panels c and d show SEM images of the same sample.

collagen-coated fibers in the initial phase (30 min, 1 h after seeding) of cell attachment, indicating a promotion of the initial adhesion by collagen coating.²⁰ Accordingly, the positive effect of collagen coating on MSC attachment was reported by Lui et al. and Yang et al., who used PLGA and hydroxyapatite as the substrate, respectively.^{38,39} Both studies demonstrated an enhanced cell proliferation on collagen-coated substrates. In our study, similar proliferation rates of the cells are recorded for the collagen-coated and uncoated chitosan scaffolds during the cultivation time of 28 d (Figure 3). The higher cell numbers observed on the collagen-coated samples (more obvious for donor II) are caused rather by slightly enhanced adhesion and

therefore higher initial cell density than by improved proliferation. These observations indicate that the natural polymer chitosan equals collagen type I in effectiveness to promote cell proliferation.

hBMSCs of both donors showed increased LDH activity in consequence of osteogenic induction. This effect is explained by the presence of dexamethasone as a component of the differentiation media.⁴⁰ Furthermore the presence of ascorbate is known to promote cell proliferation of MSC.^{40–42} Accordingly, Machado et al. found higher proliferation rates of osteogenically induced MSC compared to noninduced MSC cultivated in chitosan-containing 3D scaffolds.⁴²

The differentiation of the stem cells into osteoblast-like cells is confirmed by the increase of ALP activity.⁴³ Low ALP activity is determined for noninduced cell fractions. In the present study, increase of ALP activity was observed for hBMSCs of both donors during cultivation on the scaffolds in the presence of osteogenic supplements, whereas ALP activity did not rise in the absence of osteogenic supplements (Figure 5). The modification with collagen had no impact on the ALP activity levels. As already noticed for proliferation, this observation is in contrast to the findings of other groups which indicate a promoting effect of collagen coating on osteogenic differentiation of MSC.^{38,39,44} Alternatively, that hints at the excellent properties of the unmodified chitosan fibers as a cell culture substrate. Further studies confirmed that chitosan supports the growth and differentiation of osteoblasts.^{45,46}

Osteogenic differentiation was furthermore demonstrated by microscopic detection of the marker osteocalcin, which is particularly located around the chitosan fibers. Similar results were obtained by cultivating murine osteoblasts on chitosan scaffolds.²⁰ Possibly, the cells directly attached to the fibers are most progressed in growth and expression of extracellular matrix. For chitosan sponges it is postulated that interactions of the positive chitosan charges and negative charges on the cell surface may enhance the cell's metabolic activity.⁴⁷ On the other hand, the localization of osteocalcin in the vicinity of the chitosan fibers may also be explained by a binding of this protein to the chitosan material after secretion from the cells.

Osteocalcin was not detected for the noninduced cell fractions. In consideration of the results on ALP activity measurements, we conclude that the chitosan scaffolds applied in our study have no stimulating influence on the osteogenic differentiation of hBMSCs in the absence of osteogenic supplements. Mineralization behavior of the cells was tested when cultivated on the uncoated as well as on collagen-coated chitosan scaffolds.

However, strong mineral incorporation in the extracellular matrix, especially for the collagen-coated scaffolds, and the limit of detection of the colorimetric assay rendered quantitative detection impossible. Mineral formation in the cell layer formed by induced hBMSCs after 28 d of cultivation on uncoated and collagen-coated chitosan scaffolds was detected by SEM and analyzed by EDX. The typical composition of the elements calcium and phosphorus characterizes hydroxyapatite, the major component of the inorganic part of bone.⁴⁸ The results correlate to matrix mineralization of murine osteoblasts cultivated on textile chitosan scaffolds.²⁰

Conclusion

The excellent suitability of textile chitosan fiber scaffolds for application in bone tissue engineering was demonstrated by good adhesion, proliferation, and osteogenic differentiation of hBMSCs. Our *in vitro* experiments suggest that coating of textile chitosan scaffolds with collagen type I, a common strategy for biologization of implant materials, is not necessary to achieve acceptable biocompatibility. This observation indicates that the biological performance of chitosan fibers is comparable to that of collagen type I. Nevertheless, the collagen coating of chitosan scaffolds might be advantageous in the *in vivo* situation after implantation due to a favored initial cell adhesion or interactions with other cell types, biomolecules, or components of the extracellular matrix.

Supporting Information Available. HBMSC proliferation rates and ALP activity on polystyrene culture dishes, EDX mapping of cell-formed mineral. This material is available free of charge via the Internet at <http://pubs.acs.org>.

References and Notes

- Hench, L. L.; Polak, J. M. *Science* **2002**, 295 (5557), 1014–7.
- Salgado, A. J.; Coutinho, O. P.; Reis, R. L. *Macromol. Biosci.* **2004**, 4 (8), 743–65.
- Di Martino, A.; Sitterling, M.; Risbud, M. V. *Biomaterials* **2005**, 26 (30), 5983–90.
- Kim, I. Y.; Seo, S. J.; Moon, H. S.; Yoo, M. K.; Park, I. Y.; Kim, B. C.; Cho, C. S. *Biotechnol. Adv.* **2008**, 26 (1), 1–21.
- Varum, K. M.; Myhr, M. M.; Hjerde, R. J.; Smidsrod, O. *Carbohydr. Res.* **1997**, 299 (1–2), 99–101.
- Kohn, P.; Winzler, J.; Hoffman, R. C. *J. Biol. Chem.* **1962**, 237, 304–8.
- Kurita, K. *Mar. Biotechnol. (NY)* **2006**, 8 (3), 203–26.
- Wang, J.; Chen, Y.; Ding, Y.; Wan, C. *Appl. Surf. Sci.* **2008**, doi: 10.1016/j.apsusc.2008.06.147.
- Taylor, M. S.; Daniels, A. U.; Andriano, K. P.; Heller, J. *J. Appl. Biomater.* **1994**, 5 (2), 151–7.
- Jayakumar, R.; Selvamurugan, N.; Nair, S. V.; Tokura, S.; Tamura, H. *Int. J. Biol. Macromol.* **2008**, 43 (3), 221–5.
- Manjubala, I.; Ponomarev, I.; Wilke, I.; Jandt, K. D. *J. Biomed. Mater. Res. B: Appl. Biomater.* **2008**, 84 (1), 7–16.
- Hsu, S. H.; Whu, S. W.; Hsieh, S. C.; Tsai, C. L.; Chen, D. C.; Tan, T. S. *Artif. Organs* **2004**, 28 (8), 693–703.
- Kumar, M. N.; Muzzarelli, R. A.; Muzzarelli, C.; Sashiwa, H.; Domb, A. J. *Chem. Rev.* **2004**, 104 (12), 6017–84.
- Khor, E.; Lim, L. Y. *Biomaterials* **2003**, 24 (13), 2339–49.
- Shi, C.; Zhu, Y.; Ran, X.; Wang, M.; Su, Y.; Cheng, T. *J. Surg. Res.* **2006**, 133 (2), 185–92.
- Ohkawa, K.; Cha, D.; Kim, H.; Nishida, A.; Yamamoto, H. *Macromol. Rapid Commun.* **2004**, 25, 1600–5.
- Hutmacher, D. W. *J. Biomater. Sci., Polym. Ed.* **2001**, 12 (1), 107–24.
- Gliesche, K.; Hübner, T.; Orawetz, H. *Compos. Sci. Technol.* **2003**, 63, 81–8.
- Niekraszewicz, A.; Kucharska, M.; Wawro, D.; Struszczyk, M.; Kopias, K.; Rogaczewska, A. *Fibres Text. East. Eur.* **2007**, 15, 105–9.
- Heinemann, C.; Heinemann, S.; Bernhardt, A.; Worch, H.; Hanke, T. *Biomacromolecules* **2008**, 9 (10), 2913–20.
- Phillips, A. M. *Injury* **2005**, 36 (Suppl 3), S5–7.
- Bielby, R.; Jones, E.; McGonagle, D. *Injury* **2007**, 38 (Suppl 1), S26–32.
- Owen, M. *J. Cell Sci. Suppl.* **1988**, 10, 63–76.
- Caplan, A. I. *J. Orthop. Res.* **1991**, 9 (5), 641–50.
- Pittenger, M. F.; Mackay, A. M.; Beck, S. C.; Jaiswal, R. K.; Douglas, R.; Mosca, J. D.; Moorman, M. A.; Simonetti, D. W.; Craig, S.; Marshak, D. R. *Science* **1999**, 284 (5411), 143–7.
- Bruder, S. P.; Jaiswal, N.; Haynesworth, S. E. *J. Cell. Biochem.* **1997**, 64 (2), 278–94.
- Oswald, J.; Boxberger, S.; Jorgensen, B.; Feldmann, S.; Ehninger, G.; Bornhauser, M.; Werner, C. *Stem Cells* **2004**, 22 (3), 377–84.
- Thompson, D. L.; Lum, K. D.; Nygaard, S. C.; Kuestner, R. E.; Kelly, K. A.; Gimble, J. M.; Moore, E. E. *J. Bone Miner. Res.* **1998**, 13 (2), 195–204.
- Sepp, A.; Binns, R. M.; Lechler, R. I. *J. Immunol. Methods* **1996**, 196 (2), 175–80.
- Curran, J. M.; Chen, R.; Hunt, J. A. *Biomaterials* **2006**, 27 (27), 4783–93.
- Robins, S. P. *Biochemical Markers in Bone Turnover*; Chapman and Hall: London, 1997; pp 231–50.
- Kuboki, Y.; Jin, Q.; Takita, H. *J. Bone Joint Surg. Am.* **2001**, 83-A (Suppl 1, Pt 2), S105–15.
- Agboh, O. C.; Qin, Y. *Polym. Appl. Technol.* **1997**, 8, 355–65.
- Knaul, J.; Hooper, M.; Chanyi, C.; Creber, K. A. M. *J. Appl. Polym. Sci.* **1998**, 69, 1435–44.
- Pachence, J. M. *J. Biomed. Mater. Res.* **1996**, 33 (1), 35–40.
- Douglas, T.; Heinemann, S.; Mietrach, C.; Hempel, U.; Bierbaum, S.; Scharnweber, D.; Worch, H. *Biomacromolecules* **2007**, 8 (4), 1085–92.
- Zhang, Y. Z.; Venugopal, J.; Huang, Z.-M.; Lim, C. T.; Ramakrishna, S. *Biomacromolecules* **2005**, 6, 2583–2589.
- Liu, G.; Hu, Y. Y.; Zhao, J. N.; Wu, S. J.; Xiong, Z.; Lu, R. *Chin. J. Traumatol.* **2004**, 7 (6), 358–62.
- Yang, X. B.; Bhatnagar, R. S.; Li, S.; Oreffo, R. O. *Tissue Eng.* **2004**, 10 (7–8), 1148–59.
- Jaiswal, N.; Haynesworth, S. E.; Caplan, A. I.; Bruder, S. P. *J. Cell. Biochem.* **1997**, 64 (2), 295–312.
- Choi, K. M.; Seo, Y. K.; Yoon, H. H.; Song, K. Y.; Kwon, S. Y.; Lee, H. S.; Park, J. K. *J. Biosci. Bioeng.* **2008**, 105 (6), 586–94.
- Machado, C. B.; Ventura, J. M.; Lemos, A. F.; Ferreira, J. M.; Leite, M. F.; Goes, A. M. *Biomed. Mater.* **2007**, 2 (2), 124–31.
- Hughes, F. J.; Aubin, J. E. *Culture of Cells of the Osteoblast Lineage*; Chapman and Hall: London, 1997; pp 1–49.
- Salaszyk, R. M.; Williams, W. A.; Boskey, A.; Batorsky, A.; Plopper, G. E. *J. Biomed. Biotechnol.* **2004**, 2004 (1), 24–34.
- Klokkevold, P. R.; Vandemark, L.; Kenney, E. B.; Bernard, G. W. *J. Periodontol.* **1996**, 67, 1170–1175.
- Lahiji, A.; Sohrabi, A.; Hungerford, D. S.; Frondoza, C. G. *J. Biomed. Mater. Res.* **2000**, 51, 586–95.
- Ma, J.; Wang, H.; He, B.; Chen, J. *Biomaterials* **2001**, 22, 331–6.
- Sharma, B.; Elisseeff, J. H. *Ann. Biomed. Eng.* **2004**, 32 (1), 148–59.

BM900172M